Competition between pumping and damping in microwave-assisted magnetization reversal in magnetic films

Zihui Wang,[1] Ke Sun,[1,2] Wei Tong,[1] Mingzhong Wu,[1,*] Ming Liu,[3] and Nian X. Sun[3]
[1]*Department of Physics, Colorado State University, Fort Collins, Colorado 80523, USA*
[2]*State Key Laboratory of Electronic Thin Films and Integrated Devices, University of Electronic Science and Technology of China, Chengdu, Sichuan 610054, China*
[3]*Department of Electrical and Computer Engineering, Northeastern University, Boston, Massachusetts 02115, USA*
(Received 15 September 2009; revised manuscript received 1 January 2010; published 2 February 2010)

This paper reports the demonstration of microwave-assisted magnetization reversal (MAMR) in large-damping materials and the observation of a saturation effect for the enhancement in the MAMR process. The experiments were carried out on $Fe_{70}Co_{30}$ thin films. A reduction in the switching field was observed in the presence of microwaves. The level of such a reduction depends on the frequency and power of the microwaves. With increasing the microwave duration, the switching field decreases first but then approaches a lower limit. This saturation of the switching field reduction was interpreted in terms of the pumping-damping competition. The interpretation was supported by the measurements of the switching field as a function of the microwave duration for different conditions.

DOI: 10.1103/PhysRevB.81.064402 PACS number(s): 75.60.Jk

In the presence of microwaves, magnetization reversal in magnetic materials can be realized with relatively low magnetic fields. This effect is called microwave-assisted magnetization reversal (MAMR). The MAMR effect was observed by Thirion *et al.* in 2003.[1] These authors demonstrated microwave-assisted switching in a 20-nm-diameter cobalt particle using superconducting quantum interference device techniques. Following the work by Thirion *et al.*, the MAMR effect was observed in a number of different magnetic elements.[2–14] These include (i) single-domain elements, such as micron- and submicron-sized Permalloy film elements,[2,3] Permalloy nano dots,[4] submicron cobalt particles,[5] and cobalt nanoparticles with a diameter of only 3 nm,[6] and (ii) multidomain elements, such as cobalt strips,[7] Permalloy wires,[8] Permalloy and FeCo thin films,[9–11] Permalloy layers in magnetic tunnel junctions,[12,13] and Co/Pd multilayer structures.[14] The experiments on these elements all demonstrate that the presence of microwaves can remarkably reduce the field required for magnetization reversal if the microwave frequency is close to the natural ferromagnetic resonance (FMR) frequency of the materials. The underlying mechanism for this MAMR response is as follows: the microwaves excite large-angle magnetization precession; and the large-angle precession lowers the energy barrier for the rotation reversal in single-domain elements and that for domain nucleation or domain-wall motion in multidomain materials.

The MAMR operation involves the competition between the microwave pumping and the damping process. In previous work,[1–13] the magnetic elements had relatively small damping, and one could easily have a pumping process dominant over the damping process. Likely for this reason, the effects of the damping have never been touched on. In large-damping materials, such as perpendicular recording media, however, one can expect that the pumping-damping competition plays an extremely critical role in the MAMR process. Although a clear picture is still missing on the correlation between the pumping-damping competition and the enhancement in the MAMR process, recent simulations indicate rather clearly that the level of the switching field reduction decreases with increasing the damping constant.[15,16]

This paper reports (1) the demonstration of MAMR effect in large-damping materials and (2) the observation of a saturation effect for the enhancement in the MAMR process. The experiments were carried out on $Fe_{70}Co_{30}$ thin films with an FMR absorption measurement technique.[11] A reduction in the switching field was observed in the presence of microwaves. The level of such a reduction was found to be dependent on the power and frequency of the microwave pulses. It was also observed that, with increasing the microwave duration, the switching field decreased first and then saturated to a lower limit. The experiments indicated that this saturation response was strongly associated with the competition between the pumping and damping processes.

It is important to emphasize that the $Fe_{70}Co_{30}$ thin films used had an effective damping constant as large as that in realistic perpendicular recording media.[17] It is also important to underline that the $Fe_{70}Co_{30}$ thin films had multiple domains, and the reversal in these films was realized through domain-wall motion. In light of these aspects, the results reported below have far-reaching implications for the future of microwave-assisted perpendicular recording in exchange spring media or graded media where the magnetization is switched also through domain-wall motion.[18,19]

The measurements were carried out with a ferromagnetic resonance absorption (FMR-A) technique. Figure 1 shows the schematic diagram of the experimental setup and field configuration. A film sample with an in-plane uniaxial anisotropy is positioned on top of a microstrip line, with the film side down, the substrate side up, and the easy-axis parallel to the microstrip line. A static magnetic field H is applied parallel to the easy axis. The microwave magnetic field h produced by the microstrip line is to a large degree in the plane of the film and perpendicular to the easy axis. A vector network analyzer (VNA) is used to measure the FMR response of the sample. A pulse generator and a microwave source are

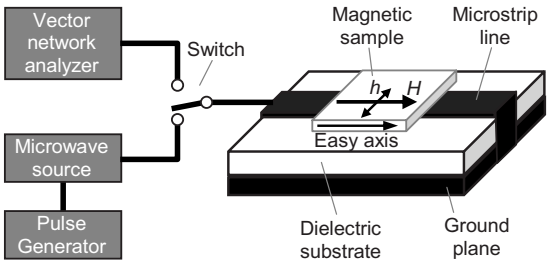

FIG. 1. Schematic diagram of experimental setup and field configuration.

used to provide microwave pulses to assist switching.

The determination of the switching field H_{sw} of the sample involves the following VNA measurements and considerations. (1) The reflection coefficient R_0 vs frequency f response of the sample-microstrip line structure is measured for a high static field ($H \gg H_{sw}$). This signal $R_0(f)$ will be used as a reference signal for subsequent measurements. (2) The reflection coefficient vs frequency response, $R(f)$, is then measured at a relatively low field. (3) The difference $R_0(f)-R(f)$ shows a peak response which results from the FMR absorption in the sample. (4) The level of the peak absorption A is measured for different static fields. (5) The A vs H profile shows a dip, and the corresponding field is the switching field. Detailed information about this technique can be found in Ref. 11.

For the MAMR measurements, one applies microwave pulses to the microstrip line before each measurement of A. Note that during the VNA measurements the power level of the microwave signal from the network analyzer is kept very low so that the MAMR response is solely due to the high-power microwave pulses. Note also that the repetition rate of the microwave pulses is very low in order to eliminate any heating effects in the sample.

The data presented below were obtained with two $Fe_{70}Co_{30}$ film samples: sample I is a 3.9×3.5 mm element, and sample II is a 3.9×3.8 mm element. The thickness was about 200 nm for both films. The films were deposited on glass substrates by dc magnetron sputtering. During the sputtering, a static magnetic field of about 250 Oe was applied to induce an in-plane uniaxial anisotropy in the films. The films were prepared under the same sputtering conditions except for the sputtering power density, which was about 15 W/cm^2 for sample I and about 5 W/cm^2 for sample II.

The films have very similar coercivities but significantly different damping properties. The easy-axis coercivity for sample I is 79 Oe, and that for sample II is 83 Oe. These values were measured with superconducting quantum interference device (SQUID) techniques and were confirmed by vibrating sample magnetometer and FMR-A measurements. The easy-axis and hard-axis FMR responses were measured with a reflection cavity microwave spectrometer. The half-power linewidths for samples I and II are about 1.40 and 2.05 kOe, respectively, at 17.3 GHz. These linewidths correspond to effective damping constants of about 0.113 and 0.166, respectively. The difference in linewidth results from the difference in the sputtering power level. In general, the FMR linewidths of metallic films consist of contributions

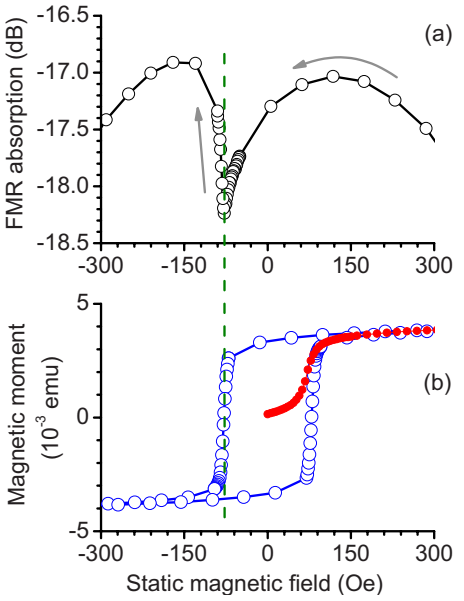

FIG. 2. (Color online) (a) A FMR absorption versus static field profile and (b) a magnetization curve and a hysteresis loop for sample I.

from intrinsic Gilbert damping, two-magnon scattering processes, and inhomogeneity line broadening.[17,20,21] It is believed that the sputtering power density has a substantial influence on the microstructure of the $Fe_{70}Co_{30}$ films, and the microstructure properties of the films play a critical role in both the two-magnon scattering and inhomogeneity line broadening. The FMR measurements also allowed for the estimation of effective anisotropy fields of the samples. For sample I, the static and dynamic components of the anisotropy field were about 20 and 209 Oe, respectively. For sample II, the static and dynamic components were about 79 and 261 Oe, respectively. The estimation used a saturation induction of $4\pi M_s=24$ kG and a gyromagnetic ratio of $|\gamma|=2.8$ MHz/Oe. The details on the separation of the static and dynamic anisotropy can be found in Ref. 22.

Figure 2 shows representative data that demonstrate the measurement of the switching field with the FMR-A approach. The data were measured on sample I with the magnetic fields along the easy axis. Graph (a) shows the A vs H profile. Graph (b) shows a magnetization curve and a hysteresis loop measured by SQUID techniques. The arrows in (a) indicate the direction of the change in field. The vertical dashed line indicates the field position of the dip in (a).

The A vs H profile in (a) shows a well-defined dip at a field that perfectly matches the coercivity of the sample. This clearly demonstrates the feasibility of the use of the FMR-A approach to measure the switching field H_{sw}. The low absorption level around H_{sw} is mainly due to the broadening of the overall resonance that results from the demagnetization or unsaturated state of the sample.[11] At the high-field ends, both positive and negative, the absorption decreases with the field. This is because the sample is saturated in these field ranges. It is well known that, in saturated materials, the FMR linewidth generally increases with field.[23,24] In (b), the magnetization curve and the hysteresis loop reach the saturation

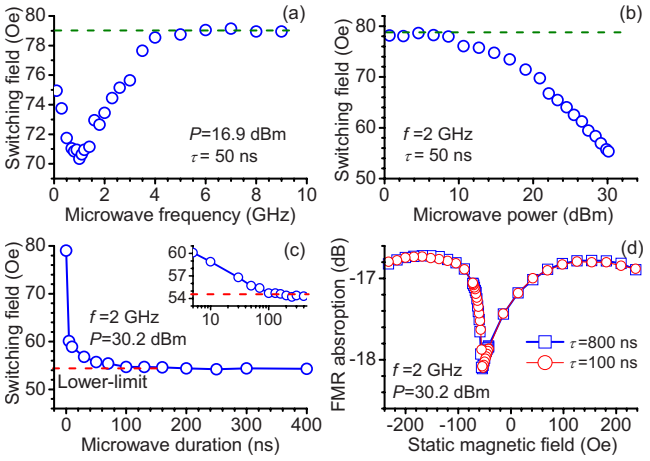

FIG. 3. (Color online) Microwave-assisted switching in sample I. (a) Switching field as a function of microwave frequency. (b) Switching field as a function of microwave power. (c) Switching field as a function of microwave duration. The inset shows the same data with the microwave duration in a logarithmic scale. (d) Two FMR absorption vs field profiles for different microwave durations, as indicated. The microwave power (P), duration (τ), and frequency (f) for the measurements are given in the graphs.

in the same field range. This clearly indicates that the coercivity of the sample results mainly from the pinning of the domain walls, rather than the nucleation of the domains.

Figure 3 shows representative data for the MAMR responses on sample I. Graph (a) shows the switching field as a function of the microwave frequency for a fixed microwave power level of $P=16.9$ dBm. Graph (b) shows the switching field as a function of the microwave power for a fixed microwave frequency of $f=2.0$ GHz. The microwave duration was set to 50 ns for the data in both (a) and (b). The horizontal dashed lines indicate the switching field in the absence of microwaves. Graph (c) gives the switching field as a function of the microwave duration τ. The inset presents the same data but with the duration shown in a logarithmic scale. The dashed lines indicate a lower limit of H_{sw}. Graph (d) shows the FMR absorption vs field profiles for two different microwave durations, as indicated. Both the data in (c) and (d) were obtained for $f=2.0$ GHz and $P=30.2$ dBm.

Five important results are evident in Fig. 3. (1) The H_{sw} vs f profile in (a) shows two different regimes: a clear dip around 1.0 GHz and a constant response in the frequency range from 5.0 to 9.0 GHz. These responses indicate that there exists an optimal frequency $f_{optimal}$ at which the microwave pumping is the most efficient and the switching field is the lowest. When the frequency is far away from this optimal frequency, there is no H_{sw} reduction. (2) The data in (b) show that the level of the H_{sw} reduction strongly depends on the microwave power. In more detail, for $P<9$ dBm the change in H_{sw} is negligible; while for $P>10$ dBm the switching field decreases significantly with increasing P. (3) The data in (b) also show that, in spite of the extremely large damping of the film, the reduction in H_{sw} can be substantial in the presence of high-P microwaves. For $P=30.2$ dBm, the maximum power available, the H_{sw} reduction is about 30%. (4) The data in (c) show that, with increasing τ, the switching field first decreases but then reaches a lower limit. This response indicates that there is a saturation for the H_{sw} reduction. (5) One sees a perfect match between the two FMR absorption vs field profiles in (d). This match, together with the flat response in the $\tau>100$ ns regime in (c), clearly indicate that the observed reduction in H_{sw} is not due to microwave heating effects. It is important to emphasize that, although not shown here, similar responses were obtained on sample II.

The above-presented results demonstrate (1) the microwave-assisted switching in large-damping films and (2) the saturation of the H_{sw} reduction in the MAMR process. The saturation effect can be interpreted in terms of the competition between the pumping and damping processes. Several key points are as follows. (1) One can define $P_{pumping}=CP_{mw}$ as the rate for the energy pumping from the microwaves to the magnetization precession, where C is the coupling efficiency and P_{mw} is the microwave power. (2) One then obtains the rate of the energy dissipation as $P_{damping}=CP_{mw}(1-e^{-2\eta t})$, where η is the decay rate of the precession and t is time. The details on the estimation of $P_{damping}$ can be found in the Appendix. (3) At the beginning of the process, the damping rate $P_{damping}$ is much lower than the pumping rate $P_{pumping}$, the pumping process is dominant, and the energy of the precession system increases with time. As a result, an increase in τ leads to an increase in the energy of the precession system, and the latter results in a reduction in the barrier for domain-wall motion and a corresponding reduction in the requisite switching field. (4) After a certain time, the damping rate $P_{damping}$ becomes very close to the pumping rate $P_{pumping}$ and one obtains a near balance between the pumping and damping processes. In this situation, an increase in τ cannot lead to further reduction in H_{sw}. (5) One can describe the energy of the precession system as

$$E(t)=\int_0^t (P_{pumping}-P_{damping})dt=\frac{CP_{mw}}{2\eta}(1-e^{-2\eta t}). \quad (1)$$

Equation (1) indicates a maximum energy $E_{max}=CP_{mw}/(2\eta)$ for the precession system. It is this maximum energy that determines the lower limit of H_{sw}.

The above interpretation may be tested through H_{sw} vs τ measurements for different conditions. This can be done by the verification of the following four expectations. (1) One can expect that the lower limit of H_{sw} is smaller if the microwave frequency is closer to $f_{optimal}$. This is because, when $f\approx f_{optimal}$, the coupling efficiency C is high and, therefore, the energy E_{max} is also high. (2) One can also expect that the higher the microwave power, the smaller the lower limit of H_{sw}. This is because the energy E_{max} increases with the microwave power P_{mw}. (3) Since the energy E_{max} is inversely proportional to the decay rate η, and the latter is proportional to the damping constant, one can expect that the energy E_{max} is lower and the reduction in H_{sw} is smaller in materials with larger damping. (4) Equation (1) indicates that the larger the decay rate η is, the faster the energy E saturates to E_{max}. This means that, with increasing τ, the switching field reaches its lower limit faster in large-damping materials than it does in low-damping materials.

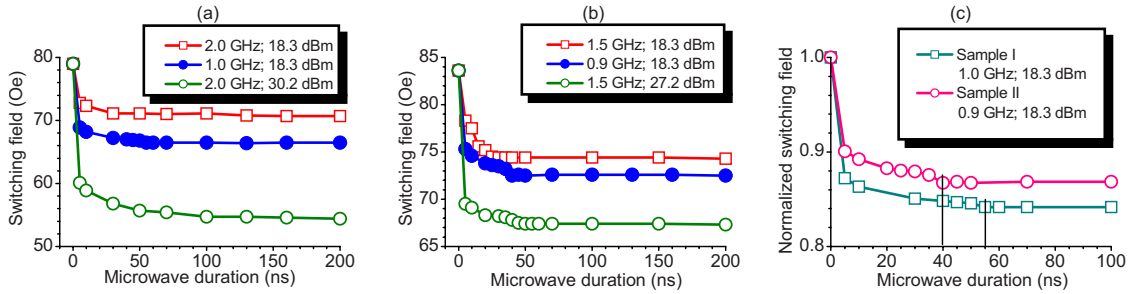

FIG. 4. (Color online) Switching field as a function of microwave duration. Graphs (a) and (b) show the data for samples I and II, respectively. Each profile shows the data obtained with different microwave signals, as indicated. Graph (c) shows the same data as in the two middle profiles in (a) and (b) with the switching fields normalized to the switching fields in the absence of microwaves.

Figure 4 gives representative H_{sw} vs τ profiles that confirm all the expectations discussed above. The data in (a) and (b) were for samples I and II, respectively. They were obtained with different microwave signals, as indicated. Graph (c) shows the same data as in the middle profiles in (a) and (b) but with the switching fields normalized to the corresponding switching fields in the absence of microwaves. The vertical lines indicate the microwave durations at which the switching fields reach their lower limits.

The top profile in (a) shows the data obtained for $f=2.0$ GHz and $P=18.3$ dBm. The data clearly indicate a H_{sw} lower limit of about 71 Oe. When one kept the microwave power unchanged but reduced the microwave frequency to the optimal frequency for MAMR operation, the limit was pushed down to about 67 Oe, as shown by the middle profile. When one kept the microwave frequency constant but raised the microwave power to 30.2 dBm, the H_{sw} lower limit decreased to about 55 Oe, as shown by the bottom profile.

Similar responses were evident in (b). In more detail, when the microwave power was set to 18.3 dBm and the microwave frequency was reduced from 1.5 to 0.9 GHz, the lower limit of H_{sw} decreased from about 74 to about 72 Oe. When the microwave frequency was kept at 1.5 GHz and the microwave power was increased from 18.3 to 27.2 dBm, the lower limit of H_{sw} decreased to about 67 Oe. Note that, although not shown here, the H_{sw} vs f profile for sample II also shows a clear dip response. This dip response indicates an optimal frequency of 0.9 GHz for sample II.

The results from (a) and (b) are in perfect agreement with expectations (1) and (2). Turn now to the data in (c). The two profiles in (c) were obtained at optimal frequencies for the same microwave power. One can see that the H_{sw} lower limit of sample I is smaller than that of sample II. One also can see that the switching fields get to their limits at about $\tau=55$ ns and $\tau=40$ ns for samples I and II, respectively. Recall that sample II has larger damping than sample I. Therefore, these results indicate that the switching field has a larger lower limit and reaches it faster in large-damping materials than it does in small-damping materials. These results agree with expectations (3) and (4).

There are three points to be noted. First, the optimal frequencies for the MAMR processes are substantially lower than the FMR frequencies estimated at the switching fields, which are about 5.3 and 7.0 GHz for samples I and II, respectively. This fact, together with the fact that the coercivity originates mainly from the pinning of domain walls, suggests the likely mechanism for the observed MAMR response: the microwaves lower the energy barrier for domain-wall motion and thereby reduce the switching field. The actual dynamics in the MAMR process, however, can be rather complicated and demands micromagnetic simulations. The spin-wave modes, for example, can be excited in the presence of the microwaves and assist the switching process.[25]

Second, the saturation effect in the H_{sw} vs τ response is surprising since one generally expects that the longer the microwave duration, the higher the energy of the precession system and the lower the switching field. In spite of the overall saturation response, the H_{sw}-τ curves do show a very small negative slope for long durations. This can be explained by the exponential dependence in Eq. (1). It might also be associated with the effect of thermal activation.[26]

Finally, in comparison with the work reported in Ref. 11, in the present work the requisite microwave power for the onset of the MAMR effect is relatively high and the switching field reduction for a given microwave power level is relatively small. The reason for these results is that the films in this work have much larger damping than the films in Ref. 11.

In summary, this paper demonstrated microwave-assisted switching in $Fe_{70}Co_{30}$ films that had effective damping constants comparable to those of perpendicular recording media. The reduction in H_{sw} with increasing τ showed a clear saturation response. The underlying mechanism for this response was explained in terms of the pumping-damping competition. The explanation was supported by the measurements of H_{sw} as a function of τ for different microwave signals and materials with different damping properties. The results from this work have far-reaching implications for microwave-assisted recording in exchange spring or graded media where the magnetization is switched also through domain-wall motion. Future demonstration of MAMR effects on realistic exchange spring or graded media is of great interest to magnetic recording.

This work was supported in part by the National Science Foundation, the Information Storage Industry Consortium, and Seagate Technology.

APPENDIX: ESTIMATION OF DAMPING RATE

Assume that the energy of the magnetization precession at time t is $E(t)$. After a very short time interval of

Δt, the energy of the precession system becomes $E(t+\Delta t)=E(t)e^{-2\eta\Delta t}+CP_{\mathrm{mw}}\Delta t$, where C is the coupling efficiency and P_{mw} is the microwave power. In this equation, the first term on the right is the decayed initial energy, and the second represents the energy from the microwave pumping. As a result, the change in energy over Δt is $\Delta E = E(t+\Delta t)-E(t)=E(t)(e^{-2\eta\Delta t}-1)+CP_{\mathrm{mw}}\Delta t$. From this energy change, one can calculate the power of the precession system at time t as $P(t)=\lim_{\Delta t\to 0}(\frac{\Delta E}{\Delta t})=CP_{\mathrm{mw}}-2\eta\frac{dP(t)}{dt}$. The solution of this equation is $P(t)=CP_{\mathrm{mw}}e^{-2\eta t}$. Since $P(t)=P_{\mathrm{pumping}}(t)-P_{\mathrm{damping}}(t)$ and $P_{\mathrm{pumping}}(t)=CP_{\mathrm{mw}}$, one obtains the damping rate as $P_{\mathrm{damping}}=CP_{\mathrm{mw}}(1-e^{-2\eta t})$.

*Corresponding author; mwu@lamar.colostate.edu

[1] C. Thirion, W. Wernsdorfer, and D. Mailly, Nature Mater. **2**, 524 (2003).

[2] G. Woltersdorf and C. H. Back, Phys. Rev. Lett. **99**, 227207 (2007).

[3] Y. Nozaki, K. Tateishi, and K. Matsuyama, Appl. Phys. Express **2**, 033002 (2009).

[4] H. T. Nembach, H. Bauer, J. M. Shaw, M. Schneider, and T. J. Silva, Appl. Phys. Lett. **95**, 062506 (2009).

[5] Y. Nozaki, M. Ohta, S. Taharazako, K. Tateishi, S. Yoshimura, and K. Matsuyama, Appl. Phys. Lett. **91**, 082510 (2007).

[6] C. Raufast, A. Tamion, E. Bernstein, V. Dupuis, Th. Tournier, Th. Crozes, E. Bonet, and W. Wernsdorfer, IEEE Trans. Magn. **44**, 2812 (2008).

[7] J. Grollier, M. V. Costache, C. H. van der Wal, and B. J. van Wees, J. Appl. Phys. **100**, 024316 (2006).

[8] Y. Nozaki, K. Tateishi, S. Taharazako, M. Ohta, S. Yoshimura, and K. Matsuyama, Appl. Phys. Lett. **91**, 122505 (2007).

[9] H. T. Nembach, P. M. Pimentel, S. J. Hermsdoerfer, B. Hillebrands, and S. O. Demokritov, Appl. Phys. Lett. **90**, 062503 (2007).

[10] P. Martín Pimentel, B. Leven, B. Hillebrands, and H. Grimm, J. Appl. Phys. **102**, 063913 (2007).

[11] C. Nistor, K. Sun, Z. Wang, M. Wu, C. Mathieu, and M. Hadley, Appl. Phys. Lett. **95**, 012504 (2009).

[12] T. Moriyama, R. Cao, J. Q. Xiao, J. Lu, X. R. Wang, Q. Wen, and H. W. Zhang, Appl. Phys. Lett. **90**, 152503 (2007).

[13] T. Moriyama, R. Cao, J. Q. Xiao, J. Lu, X. R. Wang, Q. Wen, and H. W. Zhang, J. Appl. Phys. **103**, 07A906 (2008).

[14] Y. Nozaki, N. Narita, T. Tanaka, and K. Matsuyama, Appl. Phys. Lett. **95**, 082505 (2009).

[15] J. G. Zhu, X. Zhu, and Y. Tang, IEEE Trans. Magn. **44**, 125 (2008).

[16] Z. Wang and M. Wu, J. Appl. Phys. **105**, 093903 (2009).

[17] P. Krivosik, S. Kalarickal, N. Mo, S. Wu, and C. E. Patton, Appl. Phys. Lett. **95**, 052509 (2009).

[18] M. A. Bashir, T. Schrefl, J. Dean, A. Goncharov, G. Hrkac, S. Bance, D. Allwood, and D. Suess, IEEE Trans. Magn. **44**, 3519 (2008).

[19] S. Li, B. Livshitz, H. N. Bertram, M. Schabes, T. Schrefl, E. E. Fullerton, and V. Lomakin, Appl. Phys. Lett. **94**, 202509 (2009).

[20] N. Mo, J. Hohlfeld, M. ul Islam, C. S. Brown, E. Girt, P. Krivosik, W. Tong, A. Rebei, and C. E. Patton, Appl. Phys. Lett. **92**, 022506 (2008).

[21] S. S. Kalarickal, P. Krivosik, J. Das, K. S. Kim, and C. E. Patton, Phys. Rev. B **77**, 054427 (2008).

[22] R. Lopusnik, J. P. Nibarger, T. J. Silva, and Z. Celinski, Appl. Phys. Lett. **83**, 96 (2003).

[23] A. G. Gurevich and G. A. Melkov, *Magnetization Oscillations and Waves* (CRC, New York, 1996).

[24] B. Kuanr, R. E. Camley, and Z. Celinski, Appl. Phys. Lett. **87**, 012502 (2005).

[25] R. Yanes, R. Rozada, F. Garcia-Sanchez, O. Chubykalo-Fesenko, P. M. Pimentel, B. Leven, and B. Hillebrands, Phys. Rev. B **79**, 224427 (2009).

[26] M. P. Sharrock, J. Appl. Phys. **76**, 6413 (1994).